PAPER *Special Section on Signal Processing on Irregular Sampling Grids*

Design of Two Channel Biorthogonal Graph Wavelet Filter Banks with Half-Band Kernels

Xi ZHANG[†a)], ***Senior Member***

SUMMARY In this paper, we propose a novel design method of two channel critically sampled compactly supported biorthogonal graph wavelet filter banks with half-band kernels. First of all, we use the polynomial half-band kernels to construct a class of biorthogonal graph wavelet filter banks, which exactly satisfy the PR (perfect reconstruction) condition. We then present a design method of the polynomial half-band kernels with the specified degree of flatness. The proposed design method utilizes the PBP (Parametric Bernstein Polynomial), which ensures that the half-band kernels have the specified zeros at $\lambda = 2$. Therefore the constraints of flatness are satisfied at both of $\lambda = 0$ and $\lambda = 2$, and then the resulting graph wavelet filters have the flat spectral responses in passband and stopband. Furthermore, we apply the Remez exchange algorithm to minimize the spectral error of lowpass (highpass) filter in the band of interest by using the remaining degree of freedom. Finally, several examples are designed to demonstrate the effectiveness of the proposed design method.

key words: *graph signal processing, graph wavelets, biorthogonal graph filter bank, polynomial half-band kernel, Remez exchange algorithm, flatness*

1. Introduction

Graph signal processing has a wide range of applications such as biological, energy, social, sensor, transportation networks and so on [7], [8]. Graph signal processing aims to extend the classical signal processing concepts and methodologies to signals defined on general graphs. Major challenges are how to efficiently analyze, compress and process large amounts of graph signals. In the classical signal processing theory, it is known that wavelets can provide a sparse representation of signals as a widely used signal processing tool [1]–[3]. In recent years, there are many works to extend the classical wavelet transforms to graph signals, namely, graph wavelet transforms [9]–[26]. However, a drawback is that those transforms proposed in [9]–[11] and [14] are not critically sampled. Critical sampling is important for compact representation of signals, e.g., compression. Two channel critically sampled graph wavelet filter banks have been proposed in [12], [13], [15], [17], [20]–[26] also. Furthermore, the graph filters are required to be compactly supported in the graph, i.e., the output at each vertex is computed exactly from the signal at that vertex and its K-hop neighborhood. It can be achieved by a polynomial approximation of the desired spectral kernel. The lifting-based graph wavelet filter banks in [12] and [13] are compactly supported, but not orthogonal. Two channel orthogonal graph wavelet filter banks *graph-QMF*s have been proposed in [15], but the conditions of PR (perfect reconstruction) and orthogonality cannot be exactly achieved by using the polynomial approximation of kernel filters. Narang and Ortega have proposed a simple design technique based on the Meyer's wavelet construction to obtain near orthogonal *graph-QMF*s in [15], but the reconstruction error cannot be directly controlled and may be quite large. In [21], Tay and Lin have proposed a constrained optimization method to minimize the reconstruction error of *graph-QMF*s, which used the PBP (Parametric Bernstein Polynomial) for generating the initial solution needed in the optimization. In [20], *graph-QMF*s with flatness constraints have been discussed also, where only one extra parameter was used to reduce the reconstruction error. In [25], we have also proposed a new design method to minimize the reconstruction error of graph wavelet filter banks with the specified degree of flatness. In [17], Narang and Ortega have also proposed two channel compactly supported biorthogonal graph wavelet filter banks *graphBior* by relaxing the condition of orthogonality, and given a design method based on the Cohen-Daubechies-Feauveau's wavelet construction of factorizing the maximally flat half-band filter. However, the spectral responses of the resulting graph filters are poor. In [23], Tay and Zhang have used the notion of polyphase representation and ladder structures adapted to graph filter banks to construct a class of biorthogonal graph filter banks, and used the modified PBP as half-band kernels, where the half-band kernel with the the specified degree of flatness, but lowpass (highpass) spectral filter, was designed in the least squares sense. In [24] and [26], the techniques for converting the classical wavelet filter banks to graph wavelet filter banks have been proposed also, which is an alternative to the direct design of graph wavelet filter banks. However, the resulting spectral filters are not polynomials by using the direct linear mapping of the frequency variable ω to the spectral variable λ in [24]. When the spectral filters are approximated to polynomials, the PR condition cannot be exactly satisfied, especially if the degree of polynomial is lower. In addition, the resulting spectral filters are polynomials by using the conversion technique in [26], but the spectral responses are dependent on both the mapping function and the frequency responses of classical wavelet filters.

In this paper, we propose a novel direct design method of critically sampled compactly supported biorthogonal graph wavelet filter banks with half-band kernels. First of all, we

Manuscript received November 28, 2016.
Manuscript revised March 14, 2017.

[†]The author is with the Department of Communication Engineering and Informatics, University of Electro-Communications, Chofu-shi, 182-8585 Japan.
a) E-mail: zhangxi@uec.ac.jp

DOI: 10.1587/transfun.E100.A.1743

use the polynomial half-band kernels to construct a class of biorthogonal graph wavelet filter banks, where the PR condition is structurally satisfied. Then we present a design method of the polynomial half-band kernel with the specified degree of flatness, in which the PBP is utilized to ensure that the polynomial half-band kernel has the specified zeros at $\lambda = 2$. Furthermore, we apply the Remez exchange algorithm to minimize the spectral error of lowpass (highpass) filter in the band of interest by using the remaining degree of freedom. It is well-known that the Remez exchange algorithm is an efficient approach for designing FIR linear phase filters with the equiripple magnitude response. The Remez exchange algorithm has been also used to design FIR linear phase half-band filters in [6]. In the proposed design method, a set of coefficients is easily obtained only by solving a system of linear equations, and the optimal solution is attained through a few iterations. Therefore, the proposed design algorithm is computationally efficient. Finally, several design examples are shown to demonstrate the effectiveness of the design method proposed in this paper.

2. Preliminaries

We firstly give a brief review of signal processing on graphs in [7], [8] and [15]. A graph is denoted as $G = (\mathcal{V}, E)$, where $\mathcal{V}$ is the set of vertices (nodes) and E is the set of edges (links). The size of graph $N = |\mathcal{V}|$ is the number of vertices. $\mathbf{A}$ is the adjacency matrix, whose element $A(i, j)$ represents the weight of the edge between vertex i and j, and $A(i, j) = 0$ if there is no edge. $\mathbf{D} = \mathrm{diag}(d_i)$ is the diagonal degree matrix, where $d_i = \sum_j A(i, j)$ is the sum of weights of all edges connected to vertex i. The Laplacian matrix of the graph is defined as $\mathbf{L} = \mathbf{D}-\mathbf{A}$, and the normalized Laplacian matrix is $\mathcal{L} = \mathbf{D}^{-1/2}\mathbf{L}\mathbf{D}^{-1/2} = \mathbf{I} - \mathbf{D}^{-1/2}\mathbf{A}\mathbf{D}^{-1/2}$, where $\mathbf{I}$ is the identity matrix. Both $\mathbf{L}$ and $\mathcal{L}$ are symmetric positive semidefinite matrices, and have a complete set of orthonormal eigenvectors. Now we denote the eigenvectors of the normalized Laplacian matrix $\mathcal{L}$ by $\mathbf{u}_i = [u_i(1), u_i(2), \cdots, u_i(N)]^T$ and the associated eigenvalues by λ_i, where $u_i(n)$ is real-valued and $0 = \lambda_1 < \lambda_2 \le \cdots \le \lambda_N \le 2$.

A graph signal is a function defined on the graph and the sample value $f(n)$ at vertex n can be represented as a vector $\mathbf{f} = [f(1), f(2), \cdots, f(N)]^T$. The graph Fourier transform (GFT) is defined as the projections of a signal $\mathbf{f}$ on the graph onto the eigenvectors;

$$F(\lambda_i) = \mathbf{f}^T\mathbf{u_i} = \sum_{n=1}^{N} f(n)u_i(n) \tag{1}$$

and the inverse graph Fourier transform (IGFT) is given by

$$f(n) = \mathbf{F}^T\mathbf{U}(n) = \sum_{i=1}^{N} F(\lambda_i)u_i(n) \tag{2}$$

where $\mathbf{F} = [F(\lambda_1), F(\lambda_2), \cdots, F(\lambda_N)]^T$ and $\mathbf{U}(n) = [u_1(n), u_2(n), \cdots, u_N(n)]^T$.

A filtering operation of a signal $\mathbf{f}$ in the vertex domain can be expressed in the matrix form as $\mathbf{y} = \mathbf{H}\mathbf{f}$, where $\mathbf{y} = [y(1), y(2), \cdots, y(N)]^T$ is output signal and $\mathbf{H}$ is the transform matrix of the filter given by

$$\mathbf{H} = \sum_{i=1}^{N} H(\lambda_i)\mathbf{u}_i\mathbf{u}_i^T \tag{3}$$

where $H(\lambda)$ is the spectral kernel of the filter.

By using GFT, we have in the spectral domain

$$Y(\lambda_i) = H(\lambda_i)F(\lambda_i) \tag{4}$$

where $Y(\lambda_i)$ is the GFT of output signal $\mathbf{y}$.

If the kernel filter $H(\lambda_i)$ is a polynomial of degree K,

$$H(\lambda_i) = \sum_{k=0}^{K} a_k\lambda_i^k, \tag{5}$$

we then have

$$\begin{aligned} y(n) &= \sum_{i=1}^{N} F(\lambda_i)H(\lambda_i)u_i(n) \\ &= \sum_{m=1}^{N} f(m)\sum_{k=0}^{K} a_k\sum_{i=1}^{N}\lambda_i^k u_i(m)u_i(n), \\ &= \sum_{m=1}^{N} f(m)\sum_{k=0}^{K} a_k(\mathcal{L}^k)_{n,m} \end{aligned} \tag{6}$$

where a_k are real-valued filter coefficients. Note that $(\mathcal{L}^k)_{n,m} = 0$ when the shortest path distance between vertices n and m is greater than k. Therefore, the output signal at vertex n is a linear combination of the components of input signal at vertices within a K-hop local neighborhood of vertex n. It is known in [15] and [17] that it can be implemented iteratively with K one-hop operations at each vertex without any matrix diagonalization.

3. Graph Wavelet Filter Banks

The two channel graph wavelet filter bank $\{\mathbf{H}_k, \mathbf{G}_k\}_{k=0,1}$ proposed in [15] is shown in Fig. 1. The corresponding transform matrices are given by

$$\begin{cases} \mathbf{H}_k = \sum_{i=1}^{N} H_k(\lambda_i)\mathbf{u}_i\mathbf{u}_i^T \\ \mathbf{G}_k = \sum_{i=1}^{N} G_k(\lambda_i)\mathbf{u}_i\mathbf{u}_i^T \end{cases} \tag{7}$$

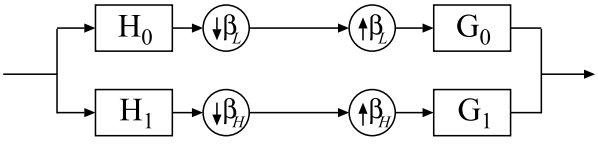

Fig. 1 Two channel graph wavelet filter bank.

where $H_k(\lambda), G_k(\lambda)$ are the spectral kernels of analysis and synthesis filters, respectively. $\mathbf{H}_0, \mathbf{G}_0$ act as lowpass filters and $\mathbf{H}_1, \mathbf{G}_1$ are highpass. The down-sampling operation β_L discards the output coefficients of lowpass channel in the set H, while β_H discards the output coefficients of highpass channel in the set L, where $|H| + |L| = N$ and $H \cap L = 0$. The overall transform matrix of the filter bank is given by

$$\begin{aligned}\mathbf{T} &= \frac{1}{2}\{\mathbf{G}_0(\mathbf{I}+\mathbf{J}_\beta)\mathbf{H}_0 + \mathbf{G}_1(\mathbf{I}-\mathbf{J}_\beta)\mathbf{H}_1\} \\ &= \frac{1}{2}\{(\mathbf{G}_0\mathbf{H}_0 + \mathbf{G}_1\mathbf{H}_1) + (\mathbf{G}_0\mathbf{J}_\beta\mathbf{H}_0 - \mathbf{G}_1\mathbf{J}_\beta\mathbf{H}_1)\}\end{aligned} \tag{8}$$

where $\mathbf{J}_\beta = \mathrm{diag}(\beta_i)$ is a diagonal matrix, and β_i is a partition function such that $\beta_i = 1$ if vertex $i \in L$ and $\beta_i = -1$ if vertex $i \in H$. Thus the down-and-up sampling operation β_L in lowpass channel can be expressed in the matrix form as $\frac{1}{2}(\mathbf{I}+\mathbf{J}_\beta)$, while β_H in highpass channel as $\frac{1}{2}(\mathbf{I}-\mathbf{J}_\beta)$.

It is shown in [15] and [17] that the PR condition of two channel graph wavelet filter banks is given by

$$\begin{cases}\mathbf{G}_0\mathbf{H}_0 + \mathbf{G}_1\mathbf{H}_1 = 2\mathbf{I} \\ \mathbf{G}_0\mathbf{J}_\beta\mathbf{H}_0 - \mathbf{G}_1\mathbf{J}_\beta\mathbf{H}_1 = \mathbf{0}\end{cases} \tag{9}$$

wnere $\mathbf{0}$ is the zero matrix. From Eq. (7), we have

$$\mathbf{G}_0\mathbf{H}_0 + \mathbf{G}_1\mathbf{H}_1 = \sum_{i=1}^{N}\{G_0(\lambda_i)H_0(\lambda_i) + G_1(\lambda_i)H_1(\lambda_i)\}\mathbf{u}_i\mathbf{u}_i^T \tag{10}$$

and since $(2-\lambda_i)$ is also an eigenvalue of $\mathcal{L}$ if λ_i is a unique eigenvalue of $\mathcal{L}$ in a bipartite graph with eigenvector [15];

$$\mathbf{u}_{(2-\lambda_i)} = \pm\mathbf{J}_\beta\mathbf{u}_{\lambda_i}, \tag{11}$$

then,

$$\mathbf{G}_0\mathbf{J}_\beta\mathbf{H}_0 - \mathbf{G}_1\mathbf{J}_\beta\mathbf{H}_1 = \sum_{i=1}^{N}\{G_0(\lambda_i)H_0(2-\lambda_i) - G_1(\lambda_i)H_1(2-\lambda_i)\}\mathbf{u}_i\mathbf{u}_i^T\mathbf{J}_\beta. \tag{12}$$

Therefore the PR condition in Eq. (9) becomes

$$\begin{cases}H_0(\lambda)G_0(\lambda) + H_1(\lambda)G_1(\lambda) = 2 \\ H_0(2-\lambda)G_0(\lambda) - H_1(2-\lambda)G_1(\lambda) = 0\end{cases} \tag{13}$$

To cancel aliasing, synthesis kernels are chosen as

$$\begin{cases}G_0(\lambda) = H_1(2-\lambda) \\ G_1(\lambda) = H_0(2-\lambda)\end{cases}. \tag{14}$$

Thus the PR condition in Eq. (13) is reduced to

$$H_0(\lambda)H_1(2-\lambda) + H_0(2-\lambda)H_1(\lambda) = 2 \tag{15}$$

which leads to a biorthogonal graph wavelet filter bank.

Furthermore, defining the product filter $P(\lambda)$ as

$$P(\lambda) = H_0(\lambda)H_1(2-\lambda), \tag{16}$$

thus Eq. (15) becomes

$$P(\lambda) + P(2-\lambda) = 2. \tag{17}$$

It is known in [17] that $P(\lambda)$ should be a half-band kernel and an odd degree polynomial to satisfy Eq. (17). It is also a lowpass kernel since $H_0(\lambda)$ and $G_0(\lambda) = H_1(2-\lambda)$ are lowpass. Moreover, if orthogonal graph wavelet filter banks are needed, the condition of $G_0(\lambda) = H_0(\lambda)$ must be imposed. However, it is known in [15] that the conditions of PR and orthogonality cannot be exactly achieved by using a polynomial approximation of kernel filters.

4. Design of Biorthogonal Graph Wavelet Filter Banks

It is known in [15] and [17] that if the spectral kernel is a polynomial of degree K, then the graph filter is exactly K-hop localized and can be implemented iteratively with K one-hop operations at each vertex without any matrix diagonalization. In this paper, we will discuss the polynomial approximation of the desired kernels.

4.1 Construction with Half-Band Kernel

In this subsection, we firstly discuss the design of lowpass kernel $H_0(\lambda)$. We construct $H_0(\lambda)$ using $Q_0(\lambda)$ as

$$H_0(\lambda) = \frac{1}{\sqrt{2}}(1 + Q_0(\lambda)) \tag{18}$$

and

$$Q_0(\lambda) = \sum_{k=0}^{K_0} a_{0k}(\lambda - 1)^{2k+1} \tag{19}$$

where the degree of polynomial $Q_0(\lambda)$ is $2K_0 + 1$ and a_{0k} are real-valued coefficients.

Since $Q_0(\lambda) = -Q_0(2-\lambda)$, we have

$$H_0(\lambda) + H_0(2-\lambda) = \sqrt{2} \tag{20}$$

which means that $H_0(\lambda)$ defined in Eq. (18) is a polynomial half-band kernel.

Next, we construct the highpass kernel $H_1(\lambda)$ using $Q_1(\lambda)$ as

$$H_1(\lambda) = \sqrt{2} - Q_1(\lambda)H_0(\lambda) \tag{21}$$

and

$$Q_1(\lambda) = \sum_{k=0}^{K_1} a_{1k}(\lambda - 1)^{2k+1} \tag{22}$$

where the degree of $H_1(\lambda)$ is $2(K_0 + K_1) + 2$ since that of $Q_1(\lambda)$ is $2K_1 + 1$, and a_{1k} are real-valued. Similarly, $Q_1(\lambda) = -Q_1(2-\lambda)$ is satisfied.

Therefore, we have

$$P(\lambda) = H_0(\lambda)H_1(2-\lambda) = 1 + Q_0(\lambda) + \frac{1}{2}Q_1(\lambda) - \frac{1}{2}Q_0^2(\lambda)Q_1(\lambda) \quad (23)$$

It is clear that the PR condition in Eq. (17) is always satisfied regardless of what the coefficients a_{0k} and a_{1k} of $Q_0(\lambda)$ and $Q_1(\lambda)$ are, which means that the PR condition in Eq. (17) is structurally satisfied.

4.2 Desired Spectral of Kernel Filters

For $H_0(\lambda)$ in Eq. (18) to be lowpass with the desired gain $\sqrt{2}$ in passband $[0, \lambda_p]$ and 0 in stopband $[\lambda_s, 2]$, we must have

$$Q_0(\lambda) = \begin{cases} 1 & (0 \le \lambda \le \lambda_p) \\ -1 & (\lambda_s \le \lambda \le 2) \end{cases} \quad (24)$$

where λ_p and λ_s are the cutoff frequencies of passband and stopband respectively, and $\lambda_p + \lambda_s = 2$.

Since $Q_0(\lambda)$ is antisymmetric ($Q_0(\lambda) = -Q_0(2-\lambda)$) between $[0, \lambda_p]$ and $[\lambda_s, 2]$, its desired spectral response $Q_0^d(\lambda)$ can be reduced to

$$Q_0^d(\lambda) = 1 \qquad (0 \le \lambda \le \lambda_p). \quad (25)$$

Further, $H_1(\lambda)$ in Eq. (21) should be highpass, that is, $H_1(\lambda) = 0$ in $[0, \lambda_p]$ and $H_1(\lambda) = \sqrt{2}$ in $[\lambda_s, 2]$. In $[\lambda_s, 2]$, $H_0(\lambda) = 0$, thus we have $H_1(\lambda) = \sqrt{2}$. On the other hand, since $H_0(\lambda) = \sqrt{2}$ in $[0, \lambda_p]$ ideally, then the desired spectral response $Q_1^d(\lambda)$ is the same as $Q_0^d(\lambda)$;

$$Q_1^d(\lambda) = 1 \qquad (0 \le \lambda \le \lambda_p). \quad (26)$$

However, $H_0(\lambda)$ has some spectral errors in practice. Thus we have from Eq. (21)

$$Q_1^d(\lambda) = \frac{\sqrt{2}}{H_0(\lambda)} \qquad (0 \le \lambda \le \lambda_p). \quad (27)$$

That is, the actual spectral response of $H_0(\lambda)$ should be considered in the design of $H_1(\lambda)$. In the following, we discuss the design of $Q_0(\lambda)$ and $Q_1(\lambda)$ (that is, $H_0(\lambda)$ and $H_1(\lambda)$) by using the PBP (Parametric Bernstein Polynomial).

4.3 Approximation of Half-band Kernel

The PBP (Parametric Bernstein Polynomial) was first introduced in [4], and expressed in [5] and [6] as

$$B(x) = \kappa(x) - \sum_{i=L}^{K_b} \alpha_i \kappa_i(x) \quad (28)$$

and

$$\kappa(x) = \sum_{i=0}^{K_b} \binom{2K_b+1}{i} x^i (1-x)^{2K_b+1-i} \quad (29)$$

$$\kappa_i(x) = \binom{2K_b+1}{i} \{x^i(1-x)^{2K_b+1-i} - x^{2K_b+1-i}(1-x)^i\} \quad (30)$$

where the degree of $B(x)$ is $2K_b + 1$, the coefficients α_i are real, L is integer, and $0 \le L \le K_b + 1$. It is clear that $B(x)$ is a halfband polynomial since $B(x) + B(1-x) = 1$, and $B(x)$ has L zeros at $x = 1$. If $\alpha_i = 0$ for all i, then the maximally flat response is obtained, that is, $L_{max} = K_b + 1$.

By using the PBP $B(x)$, we define

$$H_0(\lambda) = \sqrt{2}B(\frac{\lambda}{2}) = \sqrt{2}\{\kappa(\frac{\lambda}{2}) - \sum_{i=L_0}^{K_0} \alpha_{0i}\kappa_i(\frac{\lambda}{2})\} \quad (31)$$

where the degree of $H_0(\lambda)$ is $2K_0 + 1$ and thus $H_0(\lambda)$ has L_0 zeros at $\lambda = 2$. Therefore, we have from Eq. (18)

$$Q_0(\lambda) = 2B(\frac{\lambda}{2}) - 1 = 2\{\kappa(\frac{\lambda}{2}) - \sum_{i=L_0}^{K_0} \alpha_{0i}\kappa_i(\frac{\lambda}{2})\} - 1 \quad (32)$$

Next, we use the method proposed in [6] to design $H_0(\lambda)$. To obtain a sharper spectral response, we use the remaining degree of freedom for $B(\frac{\lambda}{2})$ to satisfy

$$1 - \delta \le B(\frac{\lambda}{2}) \le 1 + \delta \qquad (0 \le \lambda \le \lambda_p) \quad (33)$$

and

$$-\delta \le B(\frac{\lambda}{2}) \le \delta \qquad (\lambda_s \le \lambda \le 2) \quad (34)$$

where δ is a tolerance error.

From Eq. (32), Eqs. (33) and (34) can be reduced to

$$1 - 2\delta \le Q_0(\lambda) \le 1 + 2\delta \qquad (0 \le \lambda \le \lambda_p). \quad (35)$$

By applying the Remez exchange algorithm, we select $(M_0 + 1)$ extremal points λ_m as $\lambda_p = \lambda_0 > \lambda_1 > \cdots > \lambda_{M_0} \ge 0$, where $M_0 = K_0 - L_0 + 1$, and then formulate $Q_0(\lambda)$ as

$$Q_0(\lambda_m) = 1 - (-1)^m 2\delta. \quad (36)$$

By substituting $Q_0(\lambda)$ in Eq. (32) into Eq. (36), we derive a system of linear equations as follows;

$$\kappa(\frac{\lambda_m}{2}) - \sum_{i=L_0}^{K_0} \alpha_{0i}\kappa_i(\frac{\lambda_m}{2}) = 1 - (-1)^m\delta \quad (37)$$

which becomes

$$\sum_{i=L_0}^{K_0} \alpha_{0i}\kappa_i(\frac{\lambda_m}{2}) - (-1)^m\delta = \kappa(\frac{\lambda_m}{2}) - 1 \quad (38)$$

for $m = 0, 1, \cdots, M_0$. It is clear that there are $(M_0 + 1)$ equations with respect to $M_0 = K_0 - L_0 + 1$ unknown coefficients α_{0i} plus one error δ. Therefore, we can solve Eq. (38) to obtain a set of coefficients α_{0i}. Since the extremal points λ_m are unknown a priori, we initially select λ_m equally spaced

in $[0, \lambda_p]$, and then utilize an iteration procedure to obtain the equiripple spectral response. Since it only needs to solve a system of linear equations iteratively, the proposed design algorithm is computationally efficient.

On the other hand, the desired spectral response of $Q_1(\lambda)$ is dependent on $H_0(\lambda)$ as shown in Eq. (27), and $H_0(\lambda)$ has some spectral errors in practice. Thus we need to consider the actual spectral response of $H_0(\lambda)$ in the design of $H_1(\lambda)$. We use the remaining degree of freedom to satisfy

$$\sqrt{2}-\delta \le H_0(\lambda)Q_1(\lambda) \le \sqrt{2}+\delta \quad (0 \le \lambda \le \lambda_p). \tag{39}$$

Similarly, we define

$$Q_1(\lambda) = 2\{\kappa(\frac{\lambda}{2}) - \sum_{i=L_1}^{K_1} \alpha_{1i}\kappa_i(\frac{\lambda}{2})\} - 1 \tag{40}$$

where the degree of $Q_1(\lambda)$ is $2K_1 + 1$. Then we apply the Remez exchange algorithm in $[0, \lambda_p]$ and formulate $Q_1(\lambda)$ as

$$H_0(\lambda_m)Q_1(\lambda_m) = \sqrt{2} - (-1)^m\delta. \tag{41}$$

where $\lambda_p = \lambda_0 > \lambda_1 > \cdots > \lambda_{M_1} \ge 0$, and $M_1 = K_1 - L_1 + 1$. Therefore, we can obtain

$$\sum_{i=L_1}^{K_1} \alpha_{1i}\kappa_i(\frac{\lambda_m}{2}) - \frac{(-1)^m}{2H_0(\lambda_m)}\delta = \kappa(\frac{\lambda_m}{2}) - \frac{1}{2} - \frac{1}{\sqrt{2}H_0(\lambda_m)} \tag{42}$$

for $m = 0, 1, \cdots, M_1$. There are $(M_1 + 1)$ equations with respect to $M_1 = K_1 - L_1 + 1$ unknown coefficients α_{1i} plus one error δ, thus we can solve Eq. (42) to obtain α_{1i}. Note that the stopband error of highpass filter $H_1(\lambda)$ is minimized regarding the actual response of $H_0(\lambda)$. The design algorithm for kernel filters is shown in detail as follows.

4.4 Design Algorithm

Procedure {Design Algorithm for Kernel Filters}

Begin

1) Read K_0, K_1, L_0, L_1, and λ_p.
2) Select initial extremal points $\tilde{\lambda}_m$ ($\lambda_p = \tilde{\lambda}_0 > \tilde{\lambda}_1 > \cdots > \tilde{\lambda}_{M_0} \ge 0$) equally spaced in $[0, \lambda_p]$.

Repeat

3) Set $\lambda_m = \tilde{\lambda}_m$ for $m = 0, 1, \cdots, M_0$.
4) Solve a system of linear equations in Eq. (38) to obtain a set of coefficients α_{0i}.
5) Find the maxima $\tilde{\lambda}_{2m-1}$ and minima $\tilde{\lambda}_{2m}$ ($\lambda_p = \tilde{\lambda}_0 > \tilde{\lambda}_1 > \cdots > \tilde{\lambda}_{M_0} \ge 0$) of $Q_0(\lambda)$ in $[0, \lambda_p]$.

Until

Satisfy the following condition for a prescribed small constant ϵ (e.g., $\epsilon = 10^{-8}$);

$$\sum_{m=1}^{M_0} |\lambda_m - \tilde{\lambda}_m| < \epsilon$$

6) Select initial extremal points $\tilde{\lambda}_m$ ($\lambda_p = \tilde{\lambda}_0 > \tilde{\lambda}_1 > \cdots > \tilde{\lambda}_{M_1} \ge 0$) equally spaced in $[0, \lambda_p]$.

Repeat

7) Set $\lambda_m = \tilde{\lambda}_m$ for $m = 0, 1, \cdots, M_1$.
8) Solve a system of linear equations in Eq. (42) to obtain a set of coefficients α_{1i}.
9) Find the maxima $\tilde{\lambda}_{2m-1}$ and minima $\tilde{\lambda}_{2m}$ ($\lambda_p = \tilde{\lambda}_0 > \tilde{\lambda}_1 > \cdots > \tilde{\lambda}_{M_1} \ge 0$) of $H_0(\lambda)Q_1(\lambda)$ in $[0, \lambda_p]$.

Until

Satisfy the following condition for a prescribed constant ϵ;

$$\sum_{m=1}^{M_1} |\lambda_m - \tilde{\lambda}_m| < \epsilon$$

End.

5. Design Examples

In this section, we present several design examples and compare their spectral responses with the conventional method *graphBior* to demonstrate the effectiveness of the design method proposed in this paper. Since the biorthogonal graph wavelet filter bank proposed in this paper is not orthogonal, we evaluate the filter bank by using the measure of orthogonality defined in [17] given as

$$\Theta = 1 - \frac{\max\{\sqrt{C(\lambda)}\} - \min\{\sqrt{C(\lambda)}\}}{\max\{\sqrt{C(\lambda)}\} + \min\{\sqrt{C(\lambda)}\}} \tag{43}$$

where

$$C(\lambda) = \frac{H_0^2(\lambda) + H_1^2(\lambda)}{2}. \tag{44}$$

Example 1: We have designed the proposed biorthogonal graph wavelet filter banks with the maximally flat half-band spectral kernels. We have chosen $K_0 = 7, 10, 15$ and $K_1 = 6$. The obtained spectral responses of $H_0(\lambda)$ and $H_1(\lambda)$ are shown in Fig. 2. For comparison, the spectral response of biorthogonal graph wavelet filter bank *graphBior*(8, 8) in [17] has also been shown in Fig. 2, where the degree of $H_0(\lambda)$ and $H_1(\lambda)$ are 16 and 15 respectively.

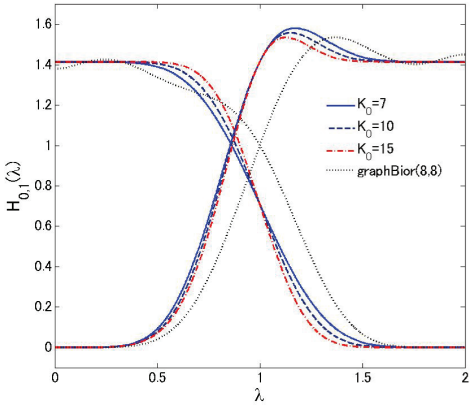

Fig. 2 Spectral responses of $H_0(\lambda)$ and $H_1(\lambda)$ in Example 1.

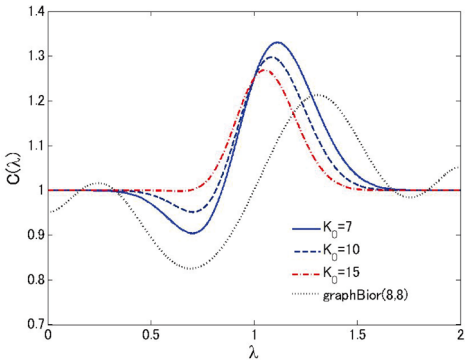

Fig. 3 Spectral responses of $C(\lambda)$ in Example 1.

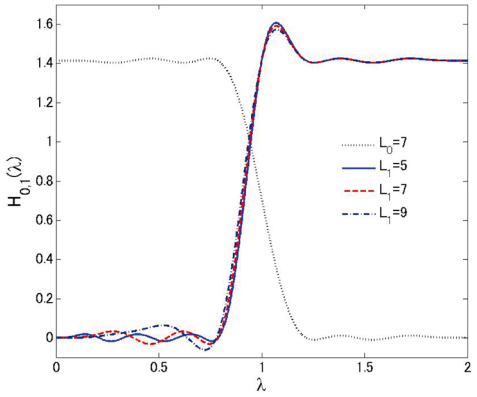

Fig. 4 Spectral responses of $H_0(\lambda)$ and $H_1(\lambda)$ in Example 2.

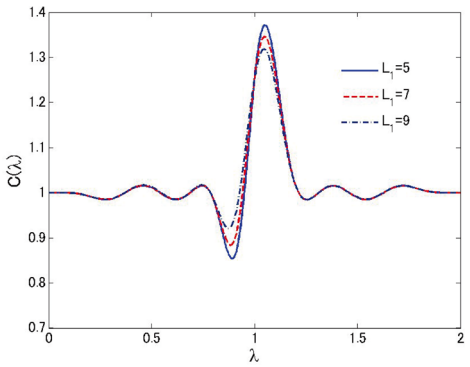

Fig. 5 Spectral responses of $C(\lambda)$ in Example 2.

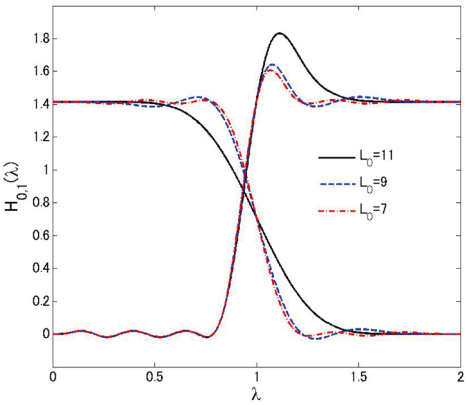

Fig. 6 Spectral responses of $H_0(\lambda)$ and $H_1(\lambda)$ in Example 3.

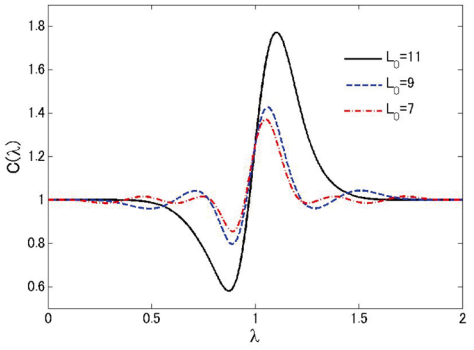

Fig. 7 Spectral responses of $C(\lambda)$ in Example 3.

It is seen that the spectral responses of the proposed filter banks are flatter at $\lambda = 0$ and $\lambda = 2$ than the *graphBior*$(8, 8)$, and become sharper nearby $\lambda = 1$ with an increasing K_0. Furthermore, the spectral responses of $C(\lambda)$ are shown in Fig. 3, and $\Theta = 0.81, 0.85, 0.88$ for $K_0 = 7, 10, 15$ whereas $\Theta = 0.81$ for *graphBior*$(8, 8)$. It is clear that the measure of orthogonality Θ becomes better with an increasing K_0.

Example 2: We have designed the biorthogonal graph wavelet filter bank with $K_0 = K_1 = 10$, and $\lambda_p = 0.8$, $\lambda_s = 1.2$. We have chosen $L_0 = 7$ and designed $H_0(\lambda)$, and then chosen $L_1 = 5, 7, 9$ to design $H_1(\lambda)$. The spectral responses of $H_0(\lambda)$ and $H_1(\lambda)$ are shown in Fig. 4. It is seen that the equiripple spectral responses of $H_0(\lambda)$ and $H_1(\lambda)$ have been obtained in the stopband by using the Remez exchange algorithm, but $H_1(\lambda)$ has an overshooting above $\lambda = 1$. The spectral responses of $C(\lambda)$ are shown in Fig. 5, and $\Theta = 0.77, 0.79, 0.82$ for $L_1 = 5, 7, 9$ respectively. It is clear that the spectral error of $H_1(\lambda)$ in the stopband becomes larger with an increasing L_1, while the measure of orthogonality Θ becomes better. Therefore, the measure of orthogonality Θ can be improved by increasing the degree L_1 of flatness of the kernel filter $H_1(\lambda)$.

Example 3: We have designed the biorthogonal graph wavelet filter bank with $K_0 = K_1 = 10$, and $\lambda_p = 0.8$, $\lambda_s = 1.2$. We have chosen $L_0 = 11, 9, 7$ and designed $H_0(\lambda)$. The spectral responses of $H_0(\lambda)$ with $L_0 = 11, 9, 7$ are shown in Fig. 6. Note that $L_0 = 11$ means the maximally flat half-band spectral kernel. It is seen that the spectral error of $H_0(\lambda)$ become smaller with a decreasing L_0. We have then designed $H_1(\lambda)$ with $L_1 = 5$, and the spectral responses of $H_1(\lambda)$ are shown in Fig. 3 also. It is seen that the equiripple spectral responses of $H_1(\lambda)$ have been obtained in the stopband. Furthermore, the spectral responses of $C(\lambda)$ are shown in Fig. 7, and $\Theta = 0.49, 0.72, 0.77$ for $L_0 = 11, 9, 7$ respectively. It is seen that the the measure of orthogonality Θ becomes better with a decreasing L_0, where Θ of the maximally flat kernel filter $H_0(\lambda)$ is the worst. Therefore, the measure of orthogonality Θ can be improved by reducing the degree L_0 of flatness of the kernel filter $H_0(\lambda)$.

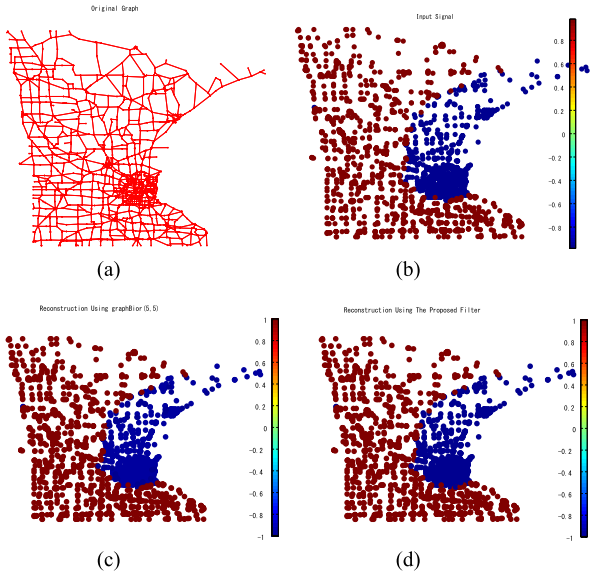

Fig. 8 (a) Minnesota traffic graph, (b) the graph signal, (c) the reconstructed signal using *graphBior*(5, 5) (SNR: 51.61 dB), and (d) the reconstructed signal using the proposed filter bank (SNR: 55.02 dB).

Example 4: To demonstrate that the graph wavelet filter banks proposed in this paper is useful in analyzing and compressing arbitrary signals defined on irregular graphs, we have applied the graph wavelet filter bank with the maximally flat half-band spectral kernels ($K_0 = 1, K_1 = 3$) to the Minnesota traffic graph signal [14], [15], [17]. The degree of $H_0(\lambda)$ and $H_1(\lambda)$ are 3 and 10 respectively. The graph is shown in Fig. 8(a), and the graph signal in Fig. 8(b), where the color of the node represents the sample value. We used the Matlab code provided in [15] and [17] to implement it. The signal is reconstructed by using a fraction of absolute-largest highpass coefficients and all of lowpass coefficients. For comparison, the compression performance of *graphBior*(5, 5) has been also investigated, where the degree of $H_0(\lambda)$ and $H_1(\lambda)$ are 10 and 9 respectively. The reconstructed signals are shown in Fig. 8(c) and 8(d), where 8% of highpass coefficients are used, and the Signal-to-Noise-Ratio (SNR) of the reconstructed graph signals are 55.02 dB for the proposed filter bank, and 51.61 dB for *graphBior*(5, 5). If 12% of highpass coefficients are used, the SNR increases to 118.74 dB and 90.23 dB respectively. It is seen that the graph wavelet filter banks proposed in this paper outperform the existing graph wavelet filter banks.

6. Conclusion

In this paper, we have proposed a new class of critically sampled compactly supported biorthogonal graph wavelet filter banks with flat spectral responses. We have used the polynomial half-band kernels to construct biorthogonal graph filter banks, which structurally safisfy the perfect reconstruction condition. We then have presented a design method for the polynomial half-band kernel, in which the PBP is utilized to ensure that the polynomial half-band kernel has the specified zeros at $\lambda = 2$. Furthermore, we have applied the Remez exchange algorithm to minimize the spectral error of lowpass (highpass) filter in the band of interest. In the proposed method, a set of coefficients can be easily obtained only by solving a system of linear equations. The optimal solution is attained through a few iterations. Therefore, the proposed design algorithm is computationally efficient. Finally, several design examples have been shown to demonstrate the effectiveness of the design method proposed in this paper.

Acknowledgments

This work was supported by JSPS KAKENHI Grant Number 26330128.

References

[1] I. Daubechies, Ten Lectures on Wavelets, SIAM, Philadelphia, PA, 1992.
[2] P.P. Vaidyanathan, Multirate Systems and Filter Banks, Prentice Hall, Englewood Cliffs, NJ, 1993.
[3] G. Strang and T. Nguyen, Wavelets and Filter Banks, Wellesley-Cambridge Press, Cambridge, MA, USA, 1996.
[4] H. Caglar and A.N. Akansu, "A generalized parametric PR-QMF design technique based on Bernstein polynomial approximation," IEEE Trans. Signal Process., vol.41, no.7, pp.2314–2321, July 1993.
[5] D.B.H. Tay, "Zero-pinning the Bernstein polynomial: A simple design technique for orthonormal wavelets," IEEE Signal Process. Lett., vol.12, no.12, pp.835–838, Dec. 2005.
[6] X. Zhang, "Design of FIR halfband filters for orthonormal wavelets using Remez exchange algorithm," IEEE Signal Process. Lett., vol.16, no.9, pp.814–817, Sept. 2009.
[7] D.I. Shuman, S.K. Narang, P. Frossard, A. Ortega, and P. Vandergheynst, "The emerging field of signal processing on graphs," IEEE Signal Process. Mag., vol.30, no.3, pp.83–98, May 2013.
[8] A. Sandryhaila and J.M.F. Moura, "Big data analysis with signal processing on graphs," IEEE Signal Process. Mag., vol.31, no.5, pp.80–90, Sept. 2014.
[9] M. Crovella and E. Kolaczyk, "Graph wavelets for spatial traffic analysis," Proc. INFOCOM 2003, vol.3, pp.1848–1857, March 2003.
[10] W. Wang and K. Ramchandran, "Random multiresolution representations for arbitrary network graphs," Proc. ICASSP 2006, vol.4, pp.161–164, May 2006.
[11] R. Coifman and M. Maggioni, "Diffusion wavelets," Appl. Comput. Harmon. Anal., vol.21, no.1, pp.53–94, 2006.
[12] G. Shen and A. Ortega, "Optimized distributed 2D transforms for irregularly sampled sensor network grids using wavelet lifting," Proc. ICASSP 2008, pp.2513–2516, April 2008.
[13] S.K. Narang and A. Ortega, "Lifting based wavelet transforms on graphs," Proc. APSIPAASC 2009, pp.441–444, Oct. 2009.
[14] D.K. Hammond, P. Vandergheynst, and R. Gribonval, "Wavelets on graphs via spectral graph theory," Appl. Comput. Harmon. Anal., vol.30, no.2, pp.129–150, 2011.
[15] S.K. Narang and A. Ortega, "Perfect reconstruction two-channel wavelet filter banks for graph structured data," IEEE Trans. Signal Process., vol.60, no.6, pp.2786–2799, June 2012.
[16] A. Sandryhaila and J.M.F. Moura, "Discrete signal processing on graphs," IEEE Trans. Signal Process., vol.61, no.7, pp.1644–1636, April 2013.
[17] S.K. Narang and A. Ortega, "Compact support biorthogonal wavelet filterbanks for arbitrary undirected graphs," IEEE Trans. Signal Process., vol.61, no.19, pp.4673–4685, Oct. 2013.
[18] A. Sandryhaila and J.M.F. Moura, "Discrete signal processing on

graphs: Frequency analysis," IEEE Trans. Signal Process., vol.62, no.12, pp.3042–3054, June 2014.
[19] Y. Tanaka and A. Sakiyama, "M-channel oversampled graph filter banks," IEEE Trans. Signal Process., vol.62, no.14, pp.3578–3590, July 2014.
[20] D.B.H. Tay and Z.P. Lin, "Graph QMF with flatness constraints," Proc. ISCAS 2015, pp.2600–2603, May 2015.
[21] D.B.H. Tay and Z.P. Lin, "Design of near orthogonal graph filter banks," IEEE Signal Process. Lett., vol.22, no.6, pp.701–704, June 2015.
[22] D.I. Shuman, C. Wiesmeyr, N. Holighaus, and P. Vandergheynst, "Spectrum-adapted tight graph wavelet and vertex-frequency frames," IEEE Trans. Signal Process., vol.63, no.16, pp.4223–4235, Aug. 2015.
[23] D.B.H. Tay and J.X. Zhang, "Techniques for constructing biorthogonal bipartite graph filter banks," IEEE Trans. Signal Process., vol.63, no.21, pp.5772–5783, Nov. 2015.
[24] A. Sakiyama, K. Watanabe, and Y. Tanaka, "Spectral graph wavelets and filter banks with low approximation error," IEEE Trans. Signal and Information Processing over Networks, vol.2, no.3, pp.230–245, Sept. 2016.
[25] X. Zhang, "Design of orthogonal graph wavelet filter banks," Proc. IECON 2016, Oct. 2016.
[26] D.B.H. Tay, Y. Tanaka, and A. Sakiyama, "Critically sampled graph filter banks with polynomial filters from regular domain filter banks," Signal Process., vol.131, pp.66–72, 2017.

Xi Zhang received the B.E. degree in electronic engineering from the Nanjing University of Aeronautics and Astronautics (NUAA), Nanjing, China, in 1984, and the M.E. and Ph.D. degrees in communication engineering from the University of Electro-Communications (UEC), Tokyo, Japan, in 1990 and 1993, respectively. He was with the Department of Electronic Engineering at NUAA from 1984 to 1987, and with the Department of Communication and Systems at UEC from 1993 to 1996, all as an Assistant Professor. He was with the Department of Electrical Engineering at Nagaoka University of Technology (NUT), Niigata, Japan, as an Associate Professor, from 1996 to 2004. Currently, he is with the Department of Communication Engineering and Informatics at UEC, as a Professor. He was a Visiting Scientist of the MEXT of Japan with the Massachusetts Institute of Technology (MIT), Cambridge, from 2000 to 2001. His research interests are in the areas of digital signal processing, graph signal processing, filter design theory, filter banks and wavelets, and its applications to image and video processing. Dr. Zhang is a senior member of the IEEE. He received the third prize of the Science and Technology Progress Award of China in 1987, and the challenge prize of Fourth LSI IP Design Award of Japan in 2002. He served as an Associate Editor for the IEEE SIGNAL PROCESSING LETTERS from 2002 to 2004.